# Codimension-two bifurcations in single-mode optical bistable systems

Hu Gang,* Cun-Zheng Ning, and H. Haken
*Institut für Theoretische Physik und Synergetik, Universität Stuttgart, Pfaffenwaldring 57/4, D-7000 Stuttgart 80, Federal Republic of Germany*
(Received 22 May 1989; revised manuscript received 6 October 1989)

The codimension-two bifurcation set of single-mode optical bistable systems is investigated. The entire set is classified into three classes, a cusp bifurcation set, a degenerate Hopf bifurcation set, and the intersection of a Hopf bifurcation and a saddle-node bifurcation. Based on the specification of degenerate Hopf bifurcation, super- and subcritical Hopf bifurcations can be identified. It is found that, in the subcritical Hopf bifurcation region, an attractor of time-dependent motion may coexist with the stable stationary solution when the cavity is filled by a passive medium. Moreover, the coexistence of three attractors is observed for certain parameter combinations.

## I. INTRODUCTION

In the past several decades, a large number of publications have focused on the study of instabilities of lasers and optical bistable systems. Many of them considered the critical condition for the onset of various instabilities. Codimension-one bifurcations, especially the Hopf-bifurcation instability, have been extensively investigated.[1–23] Recently, there appears a considerable interest in the study of multicodimension bifurcations,[24–26] since it is realized that in the close vicinity of a multicodimension bifurcation set there might appear a rich variety of characteristic behaviors including complicated chaotic motions.[27–29] Nevertheless, a systematic study in multicodimension bifurcations in an optical bistable systems is still lacking.

The aim of the present publication is to investigate the conditions for codimension-two bifurcations of a single-mode optical bistable system (SMOB). In the remainder of this section, we will present our model. For the sake of clarity, some known results closely related to this problem will be briefly described. In Sec. II the possible types and the conditions for the onset of codimension-two bifurcations of our system will be studied in detail. In Sec. III a detailed calculation to distinguish between sub- and supercritical Hopf bifurcations is carried out that, for the first time, reveals the coexistence of the stable stationary solution and a time-dependent solution, and the coexistence of three attractors in a SMOB system.

The model used is an optical unidirectional cavity filled with a medium, consisting of homogeneously broadened two-level atoms, and driven by an external coherent field. In the presentation we consider only the single-mode case, and apply the plane-wave approximation. Taking the mean-field limit,[13] we reduce the Maxwell-Bloch equations to

$$\begin{aligned} dx/dt &= -k[(1+i\theta)x - y + 2Cp] \ , \\ dp/dt &= xD - (1+i\Delta)p \ , \\ dD/dt &= -\gamma[(x^*p + xp^*)/2 + D - \sigma] \ , \end{aligned} \tag{1.1}$$

where $x,p$ are the complex output field and the atomic polarization, respectively. $D$ is the normalized real population difference. $\sigma$ is set to 1 for a passive medium and to $-1$ for an active one. [In this paper we focus on optical bistability (OB), thus $\sigma = 1$.] Equations (1.1) are essentially five dimensional. The parameter $C$ is the bistability parameter. $\gamma$ and $k$ are the longitudinal decay rate and the cavity linewidth, respectively, scaled by the transverse relaxation rate $\gamma_\perp$. The frequencies of the external field, the cavity, and the atoms are denoted by $\omega_0$, $\omega_c$, and $\omega_a$, respectively. The two detuning parameters are defined as

$$\theta = (\omega_c - \omega_0)/(k\gamma_\perp), \quad \Delta = (\omega_a - \omega_0)/\gamma_\perp \ .$$

The normalized amplitude of the external field $y$ is assumed to be real and positive.

The stationary solution of (1.1) can be worked out explicitly. It reads

$$\begin{aligned} y &= |x_s|\{[1 + 2C\sigma/(1+\Delta^2+|x_s|^2)]^2 \\ &\qquad + [\theta - 2C\Delta\sigma/(1+\Delta^2+|x_s|^2)]^2\}^{1/2} \ , \\ D_s &= (1+\Delta^2)\sigma/(1+\Delta^2+|x_s|^2) \ , \\ p_s &= (1-i\Delta)x_s\sigma/(1+\Delta^2+|x_s|^2) \ , \end{aligned} \tag{1.2}$$

The standard way to study the bifurcation set of (1.1) is to linearize (1.1) about the solution (1.2), and then to investigate the changes in the sign of the real part of the eigenvalues of the linearized equations. About (1.2) the linearized version of Eqs. (1.1) is given by

 

$$\begin{pmatrix} d\delta x/dt \\ d\delta x^*/dt \\ d\delta p/dt \\ d\delta p^*/dt \\ d\delta D/dt \end{pmatrix} = (\underline{L}) \begin{pmatrix} \delta x \\ \delta x^* \\ \delta p \\ \delta p^* \\ \delta D \end{pmatrix} = \begin{pmatrix} -k(1+i\theta) & 0 & -2Ck & 0 & 0 \\ 0 & -k(1-i\theta) & 0 & -2Ck & 0 \\ D & 0 & -(1+i\Delta) & 0 & x_s \\ 0 & D & 0 & -(1-i\Delta) & x_s \\ -rp_s^*/2 & -rp_s/2 & -rx_s^*/2 & -rx_s/2 & -r \end{pmatrix} \begin{pmatrix} \delta x \\ \delta x^* \\ \delta p \\ \delta p^* \\ \delta D \end{pmatrix}, \quad (1.3)$$

where

$$\delta x = x - x_s, \quad \delta p = p - p_s, \quad \delta D = D - D_s .$$

Equation (1.3) gives rise to the characteristic equation

$$\lambda^5 + a_1\lambda^4 + a_2\lambda^3 + a_3\lambda^2 + a_4\lambda + a_5 = 0 , \quad (1.4)$$

with

$$\begin{aligned} a_1 &= 2k + 2 + \gamma , \\ a_2 &= k^2(1+\theta^2) + (2\gamma + 1 + \Delta^2 + \gamma X^2) \\ &\quad + 2k(\gamma+2) + 4CDk , \\ a_3 &= \gamma(1+\Delta^2+X^2) + 2k(2\gamma+1+\Delta^2+\gamma X^2) \\ &\quad + k^2(1+\theta^2)(2+\gamma) + 4CDk(\gamma+k+1) \\ &\quad - 2Ck\gamma X^2/(1+\Delta^2+X^2) , \\ a_4 &= 2k\gamma(1+\Delta^2+X^2) + k(1+\theta^2)(2\gamma+1+\Delta^2+\gamma X^2) \\ &\quad + 2CDk[2k(1-\theta\Delta) + 2\gamma(k+1) + \gamma X^2] \\ &\quad - 2Ck\gamma X^2[\Delta(\Delta+\theta k) + (k+1)]/(1+\Delta^2+X^2) \\ &\quad + 4C^2D^2k^2 , \\ a_5 &= k^2\gamma\{4C^2D[D - X^2/(1+\Delta^2+X^2)] \\ &\quad + (1+\theta^2)(1+\Delta^2+X^2) + 4CD(1-\theta\Delta)\} , \end{aligned} \quad (1.5)$$

where we simply use $X$ and $D$ instead of $|x_s|$ and $D_s$, respectively. All the coefficients in (1.5) are expressed in terms of the external control parameters $C$, $\gamma$, $k$, $\Delta$, $\theta$, and $X$. (Here and in the following, we use $X$ instead of $y$ as an external control parameter.)

There are two kinds of codimension-one bifurcations. First, class $A$, a real eigenvalue of (1.4), which is the largest compared with the real part of all the other eigenvalues, changes its sign from negative to positive. The necessary condition for the bifurcation of class $A$ (i.e., saddle-node bifurcation in our case) is

$$a_5 = 0 . \quad (1.6)$$

Second, class $B$, a pair of complex conjugate eigenvalues, which have the largest real part, cross the imaginary axis, and their real parts become positive. Accordingly the necessary condition for the bifurcation of class $B$, i.e., Hopf bifurcation, reads

$$f = (a_1a_2 - a_3)(a_3a_4 - a_2a_5) - (a_1a_4 - a_5)^2 = 0 . \quad (1.7)$$

It is obvious that neither (1.6) nor (1.7) is the sufficient condition for the corresponding bifurcations. However, if we start from a stable region, the necessary and sufficient condition for the bifurcation of class $A$ is the first transversal crossing of the hypersurface (1.6), while for class $B$, it is the hypersurface (1.7). By the first crossing we mean that no other surface (1.6) or no other surface (1.7), respectively, has been crossed before the given surface is crossed. Henceforth, we call the subset of (1.6), which can be first crossed by starting from a stable region, surface $A$, and the subset of (1.7) surface $B$. Therefore, surface $A$ is the instability boundary of saddle-node bifurcation, and surface $B$ is that of Hopf bifurcation (for details, see Ref. 20).

## II. CODIMENSION-TWO BIFURCATIONS

We will classify codimension-two bifurcations of SMOB into the following four types.

### A. Type I (cusp-catastrophe bifurcation)

The best understood codimension-two bifurcation in OB is the cusp-catastrophe bifurcation in which two control parameters and one order parameter are involved. The critical parameter condition for type-I bifurcation reads

$$a_5 = 0, \quad d(a_5)/d(X^2) = 0 . \quad (2.1)$$

Of course, Eqs. (2.1) can be regarded as the cusp bifurcation set only if it is on surface $A$. (Afterwards, whenever we discuss codimension-two bifurcation, it is implied that the set involved must be either on surface $A$ or $B$, or on the intersections of both.)

At this bifurcation set, the complete unfolding of the order-parameter equation takes the form

$$dz/dt = \mu_0 + \mu_1 z + G_1 z^3 , \quad (2.2)$$

where $z$ is assumed to be the order parameter and $\mu_0$ and $\mu_1$ are small unfolding parameters. $G_1$ is a finite number. The coefficients $G_1$, $\mu_0$, $\mu_1$, and the order parameter $z$ can be explicitly calculated, according to the theory of the slaving principle.[30,31] Here, we do not intend to go further.

### B. Type II (degenerate Hopf bifurcation)

At the bifurcation set of class $B$, the unfolding of the order-parameter equations can be written as[29]

$$dr/dt=\mu r+\bar{G}_3 r^3+\bar{G}_5 r^5+\cdots ,$$
$$d\theta/dt=\omega+O(r^2) , \tag{2.3}$$

with

$$\omega^2=(a_1a_4-a_5)/(a_1a_2-a_3) \tag{2.4}$$

and $\mu$ being a small unfolding parameter. The subset of surface $B$ satisfying the conditions[32] (we shall use $G_3$ to denote $\bar{G}_3$ at the critical point where $\mu=0$)

$$f=0, \quad G_3=0 \tag{2.5}$$

is just the so-called codimension-two degenerate Hopf bifurcation set. Based on (2.5), sub- and supercritical Hopf bifurcations of SMOB can be distinguished. The condition for supercritical bifurcation reads[22,24]

$$f=0, \quad G_3<0 , \tag{2.6}$$

and that for subcritical is given by[22,24]

$$f=0, \quad G_3>0 . \tag{2.7}$$

In free-running laser systems (FRL), there have been a variety of publications analytically and numerically dealing with the problem of sub- and supercritical Hopf bifurcations.[24–26] It has been found that, for the Lorenz equations, which can be deduced from a set of FRL equations as its special case,[1] the stationary solution can undergo only subcritical Hopf bifurcation.[23] However, considering complex Lorenz equations which are just a revised version of the FRL equations,[33] both sub- and supercritical bifurcations may be observed.[33] Nevertheless, up to date, with the SMOB system the classification of sub- and supercritical bifurcations has not yet been carried out. This is an important task of the present paper. We leave the calculation of the parameter $G_3$ and the consequent classification of the super- and subcritical Hopf bifurcations to Sec. III.

### C. Type III (interaction of surfaces $A$ and $B$)

Type-I and type-II bifurcations are the simplest saddle-node bifurcation and the Hopf bifurcation with higher-order degeneracy. The numbers of the order parameters do not differ from those of the corresponding codimension-one bifurcations. Now we consider a substantially different situation.

Surfaces $A$ and $B$ may intersect each other. Moreover, various sheets of one kind of surface may intersect each other as well. For the intersection of $A$ and $B$ to occur the conditions

$$a_5=0, \quad f=0 \tag{2.8}$$

must be fulfilled simultaneously. Equations (2.8) can be satisfied by two possible ways which correspond to two classes of bifurcations of type III.

#### 1. *Type III A*

Type III A is defined by

$$a_5=0, \quad a_4=0 . \tag{2.9}$$

At an intersection of this kind, the frequency of the unstable mode is zero,

$$\omega^2=(a_1a_4-a_5)/(a_1a_2-a_3)=0 , \tag{2.10}$$

and then the mode on surface $B$ is softened about the III A set. Thus, we will call III A soft-mode intersection of $A$ and $B$. The eigenvalue equation (1.4) has the double-zero eigenvalue degeneracy

$$\lambda_1=\lambda_2=0$$

and the standard linear matrix of the order-parameter equations takes the form

$$\begin{bmatrix} 0 & 1 \\ 0 & 0 \end{bmatrix} . \tag{2.11}$$

The time-dependent problem about the bifurcation set is essentially two dimensional with two unfolding parameters involved.

#### 2. *Type III B*

Equation (2.8) can be again satisfied in the following manner:

$$a_5=0, \quad u=(a_1a_2-a_3)a_3-a_1^2a_4=0 . \tag{2.12}$$

At the bifurcation point we have simultaneously

$$\lambda_3=0, \quad \lambda_{1,2}=\pm i\omega$$

with

$$\omega^2=a_1a_4/(a_1a_2-a_3)\neq 0 . \tag{2.13}$$

Since curve $B$ is defined by the first crossing of the boundary (1.7) by the system starting from a stable region, then this curve serves as the necessary and sufficient condition for Hopf bifurcation. Thus $\omega^2$ must be nonnegative at $B$ (for the detailed discussion see Refs. 20 and 34). Point III B will be called hard-mode intersection. The standard linear matrix of the order-parameter equations reads

$$\begin{bmatrix} 0 & -\omega & 0 \\ \omega & 0 & 0 \\ 0 & 0 & 0 \end{bmatrix} . \tag{2.14}$$

In the vicinity of the bifurcation point, Eqs. (1.1) can be reduced to a set of three order-parameter equations with two unfolding parameters.

In Fig. 1 we plot a bifurcation figure of SMOB in the $x$-$\Delta$ plane by fixing $C=500$, $k=0.5$, $\gamma=2$, and $\theta=-14$. The dashed and solid curves correspond to Eqs. (1.6) and (1.7), respectively. Note that only those parts of the solid (dashed) curve which fall outside the dashed (solid) curve are called $B$ ($A$) curve in accordance with our definition. It should be understood that the dashed (solid) part inside the solid (dashed) curve is not the instability boundary of class $A$ ($B$). The areas surrounded by the dashed or solid curves are unstable regions. At points I, II, and III B we find codimension-two bifurcations of types I, II, and III, respectively. The dotted circle, defined by $u=0$, crosses all intersections of $A$ and $B$. Hence, it is clear that all intersections belong to type-III B bifurcation. We have

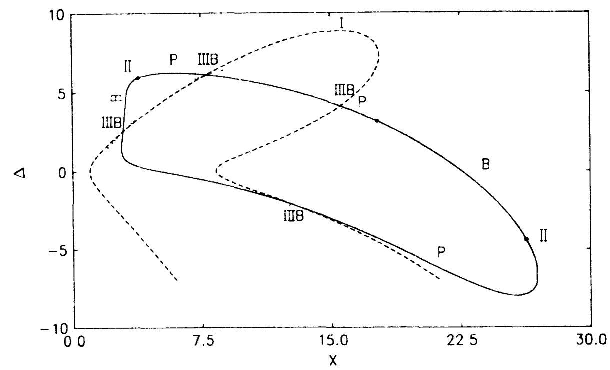


FIG. 1. $C=500$, $\gamma=2$, $k=0.5$, and $\theta=-14$. The dashed and the solid curves are defined by Eqs. (1.6) and (1.7), respectively. However, only the dashed and the solid curves separating the stable region from the unstable region are defined as the instability boundaries of classes $A$ and $B$, respectively. The dotted line, plotted according to $u=0$, crosses all the intersections of $A$ and $B$. Then III B bifurcation is verified at each intersection. At points I, II, and III B, codimension-two bifurcations of types I, II, and III B take place, respectively.

varied $C$, $k$, $\gamma$, and $\theta$ in a wide region, and no bifurcation of type III A has been found. It leads us to the suggestion that in SMOB hard-mode intersection prevails.

Both curves $A$, $B$, and their intersections can be varied by changing the remaining fixed parameters. By decreasing any one of $C$, $\gamma$, and $k$, circle $B$ can be made to contract and eventually disappear. Thus, only type I codimension-two bifurcation can survive as $k\to 0$, or $\gamma\to 0$, and none of the bifurcations, including those of codimension-one or two, remains for small enough $C$. In Fig. 2 we fix $C=75$, $k=0.5$, $\gamma=2$, and $\theta=-8$. In comparison with Fig. 1, the reduction of the unstable regions $A$ and $B$ is apparent. Note that in Fig. 2 the number of the intersections of $A$ and $B$ is only two rather than four (see Fig. 1). Surface $A$ is not altered by increasing $k$, while surface $B$ is sensitive to the change of $k$. The latter can be first enlarged and then pushed up as we increase $k$. Therefore, circle $B$ as well as all the codimension-two bifurcations other than type I will eventually disappear from the scope of Fig. 1 as $k\to\infty$.

### D. Type IV (intersection of two $B$ sheets)

Surface $B$ may contain various sheets. Different sheets might intersect each other, leading to multicodimension bifurcations. Since Eqs. (1.1) are five dimensional, one can expect only intersections of two $B$ sheets. At the bifurcation set of type IV, we have

$$\lambda_{1,2}=\pm i\omega_1,\quad \lambda_{3,4}=\pm i\omega_2\ . \tag{2.15}$$

In order for Eqs. (2.15) to be fulfilled, the two algebraic equations

$$\omega^4-a_2\omega^2+a_4=0\ , \tag{2.16a}$$

$$a_1\omega^4-a_3\omega^2+a_5=0 \tag{2.16b}$$

must have two pairs of real common solutions $\pm\omega_1$, $\pm\omega_2$ that require

$$a_1a_2-a_3=f=0\ ,$$

or equivalently,

$$a_1a_2-a_3=0\ , \tag{2.17a}$$

$$a_1a_4-a_5=0\ . \tag{2.17b}$$

It is interesting to point out that in case of SMOB, we always have

$$a_1a_2-a_3>0 \tag{2.18}$$

[cf. (1.5)], and no codimension-two bifurcation of type IV can be observed. Thus, the entire codimension-two bifurcation set of SMOB can be specified according to three classes, types I, II, and III B.

The investigation and the classification of codimension-two bifurcations of types I–III B are rather instructive. According to the understanding of the type-I bifurcation set, we are able to demonstrate the coexistence of multistationary states which are crucial to a bistable system. It is known that under certain parameter conditions[28,29] complicated motions including chaos may appear in the vicinity of the type-III B bifurcation set. Thus it might be possible to predict chaotic motion in SMOB analytically by identifying the III B codimension-two bifurcation set and by analyzing the corresponding order-parameter equations with much lower dimensions. We will deal with this matter in a forthcoming paper. In the remainder of this paper, we will give a detailed analysis of type-II bifurcation.

## III. SUB- AND SUPERCRITICAL BIFURCATIONS AND NEW ATTRACTORS IN SMOB SYSTEMS

In the following we shall follow a method of combining the elimination procedures[30,31] and the normal form theory, as we did in Refs. 24 and 33. The elimination procedures, i.e., below from (3.1) to (3.16), have been successfully used in various problems in laser-related systems

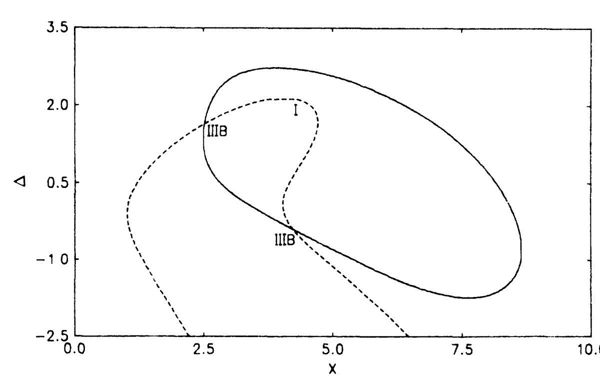


FIG. 2. The same as in Fig. 1 with $C$ and $\theta$ replaced by $C=75$, $\theta=-8$. The unstable regions surrounded by $A$ and $B$ are considerably reduced by decreasing $C$. The number of the intersections of $A$ and $B$ is reduced from four to two.

to reduce the dimension of the systems, i.e., self-pulsing in multimode lasers,[35] two-photon lasers,[24] and lasers with an injected signal.[36] The calculation of $G_3$ based on a general two-dimensional order-parameter equation has been previously undertaken for two-photon lasers, leading to an analytical criterion for the discrimination of the Hopf bifurcation nature.[24] The power and efficiency of this kind of approach have already been demonstrated.

First of all, let us define the order parameters and the coefficient $G_3$. Then sub- and supercritical bifurcations in SMOB will be distinguished by searching for the level curve $G_3=0$.

At surface $B$, Eq. (1.4) has two pure imaginary solutions [see Eq. (2.4)]

$$\lambda_{1,2}=\pm i\omega \ . \tag{3.1}$$

The other three eigenvalues can be obtained from the equation

$$\lambda^3+a_1\lambda^2+b_2\lambda+b_3=0 \ , \tag{3.2}$$

where

$$b_2=a_2-(a_1a_4-a_5)/(a_1a_2-a_3) \ ,$$
$$b_3=a_5(a_1a_2-a_3)/(a_1a_4-a_5) \ .$$

They are

$$\lambda_3=h_1+h_2, \quad \lambda_4=v_1h_1+v_2h_2, \quad \lambda_5=v_2h_1+v_1h_2 \tag{3.3}$$

with

$$v_{1,2}=(-1\pm 3i)/2 \ ,$$
$$h_{1,2}=\{-q/2\pm[(q/2)^2+(p/3)^3]^{1/2}\}^{1/3} \ ,$$
$$q=-2a_1^3/27-a_1b_2/3+b_3 \ ,$$
$$p=-a_1^2/3+b_2 \ .$$

Inserting $\lambda_1,\ldots,\lambda_5$ into Eqs. (1.3), we obtain the corresponding eigenvectors $\alpha_{ij}$, by which we can form new variables $z_i$. The new and the old variables are related through

$$\delta y_i=\sum_{j=1}^{5}(\alpha_{ij})z_j \tag{3.4}$$

with

$$\delta y_1=\delta x, \quad \delta y_2=\delta x^*, \quad \delta y_3=\delta p \ ,$$
$$\delta y_4=\delta p^*, \quad \delta y_5=\delta D \ .$$

Since it is assumed that $\lambda_{1,2}$ are the eigenvalues first crossing the real axis, then $z_1$ and $z_2$ will be the order parameters. All the remaining variables $z_3$, $z_4$, and $z_5$ correspond to the fast damped modes and can be eliminated adiabatically. However, the adiabatical elimination can be correctly performed only after we have defined all the order parameters and the fast modes. For this purpose let us calculate all the eigenvectors of the linear equations (1.3). $\alpha_{ij}$ can be explicitly given by solving

$$(\underline{L})\begin{pmatrix}\alpha_{1i}\\ \alpha_{2i}\\ \alpha_{3i}\\ \alpha_{4i}\\ \alpha_{5i}\end{pmatrix}=\lambda_i\begin{pmatrix}\alpha_{1i}\\ \alpha_{2i}\\ \alpha_{3i}\\ \alpha_{4i}\\ \alpha_{5i}\end{pmatrix} \ . \tag{3.5}$$

The results are

$$\begin{aligned}
&\alpha_{1i}=\exp(i\phi_i), \quad \alpha_{2i}=\exp(-i\phi_i) \ ,\\
&\alpha_{3i}=[-k(1+i\theta)-\lambda_i]\exp(i\phi_i)/(2Ck) \ ,\\
&\alpha_{4i}=[-k(1-i\theta)-\lambda_i]\exp(-i\phi_i)/(2Ck) \ ,\\
&\alpha_{5i}=\{D+[(1+i\Delta)+\lambda_i][k(1+i\theta)+\lambda_i]/(2Ck)\}\\
&\qquad\times\exp(i\phi_i)/x_s, \quad i=1,2,\ldots,5 \ .
\end{aligned} \tag{3.6}$$

The phase angles $\phi_i$ are defined as

$$\exp(i\phi_i)=[(x_s\{2CDk+(1-i\Delta+\lambda_i)[k(1-i\theta)+\lambda_i]\})/(x_s^*\{2CDk+(1+i\Delta)[k(1+i\theta)+\lambda_i]\})] \ . \tag{3.7}$$

We fix the arbitrary factor by choosing $\alpha_{1i}=\exp(i\phi_i)$ in order to keep the symmetry that a new variable $z_j$ corresponding to a real eigenvalue is real and a pair of new variables corresponding to the complex conjugate eigenvalues are complex conjugate.

In order to form the order-parameter equations, one must also know the inverse of the matrix $(\alpha)$ satisfying

$$(\beta)(\alpha)=I \ .$$

Then the new variables can be expressed in terms of the old ones as

$$z_i=\sum_{j=1}^{5}\beta_{ij}\delta y_j, \quad i=1,2,\ldots,5 \ . \tag{3.8}$$

There is no essential difficulty to calculate $\beta_{ij}$ from $\alpha_{ij}$. However, the explicit formulas might frequently be complicated since the matrix is five dimensional. Nevertheless, a compact explicit result of matrix $(\beta)$ can be obtained by calculating the left eigenvalue problem

$$\lambda_i(\beta'_{i1}\beta'_{i2}\beta'_{i3}\beta'_{i4}\beta'_{i5})=(\beta'_{i1}\beta'_{i2}\beta'_{i3}\beta'_{i4}\beta'_{i5})(\underline{L}) \ , \tag{3.9}$$

which gives rise to

$$\begin{aligned}
&\beta'_{i1}=\exp(i\psi_i),\quad \beta'_{i2}=\exp(-i\psi_i)\ ,\\
&\beta'_{i3}=(\{-2Ckp_s^*+x_s^*[k(1+i\theta)+\lambda_i]\}/[D_s x_s^*+p_s^*(1+i\Delta+\lambda_i)])\beta'_{i1}\ ,\\
&\beta'_{i4}=(\{-2Ckp_s+x_s[k(1-i\theta)+\lambda_i]\}/[D_s x_s+p_s(1-i\Delta+\lambda)])\beta'_{i2}\ ,\\
&\beta'_{i5}=(\{-4CkD_s-2(1+i\Delta+\lambda_i)[k(1+i\theta)+\lambda_i]\}/[\gamma D_s x_s^*+\gamma p_s^*(1+i\Delta+\lambda_i)])\beta'_{i1}\ ,\\
&\exp(i\psi_i)=\frac{(\{2CkD_s+(1-i\Delta+\lambda_i)[k(1-i\theta)+\lambda_i]\}[\gamma D_s x_s^*+\gamma p_s^*(1+i\Delta+\lambda_i)])}{(\{2CkD_s+(1+i\Delta+\lambda_i)[k(1+i\theta)+\lambda_i]\}[\gamma D_s x_s+\gamma p_s(1-i\Delta+\lambda_i)])}\ .
\end{aligned}\tag{3.10}$$

Matrix $(\beta)$ can be obtained by multiplying $(\beta')$ by normalization constants

$$\beta_{ij}=\beta'_{ij}/\beta_i,\quad \beta_i=\sum_{j=1}^{5}\beta'_{ij}\alpha_{ij},\quad i=1,2,\ldots,5\ . \tag{3.11}$$

Now Eqs. (1.1) can be reduced by taking the transformation (3.4) and (3.8) to a rather concise form

$$\begin{aligned}
dz_j/dt=&\lambda_j z_j+\beta_{j3}\delta x\,\delta D+\beta_{j4}\delta x^*\delta D\\
&-\gamma\beta_{j5}(\delta x^*\delta p+\delta x\,\delta p^*)/2\ .
\end{aligned}$$

Inserting (3.5) into the above equations, we finally arrive at

$$\begin{aligned}
dz_j/dt=\lambda_j z_j+\sum_{k,l=1}^{5}&[\beta_{j3}\alpha_{1l}\alpha_{5k}+\beta_{j4}\alpha_{3l}\alpha_{5k}\\
&-\gamma\beta_{j5}(\alpha_{2l}\alpha_{3k}+\alpha_{1l}\alpha_{4k})/2]z_l z_k\ .
\end{aligned}\tag{3.12}$$

Equations (3.12) are equivalent to Eqs. (1.1). However, the linear part of the former has a normal form, i.e., a form with no coupling of different variables in the linear part. The order parameters $z_1$ and $z_2$ are therefore well separated from the fast modes $z_3$, $z_4$, and $z_5$ in the linear regime. The elimination procedure[30,31] can be directly performed. Note that in the present case the fast modes cannot be directly eliminated by setting $dz_i/dt=0$, $i=3,4,5$, because the order parameters have finite frequencies. We assume[24]

$$z_j=B_{11}(j)z_1^2+B_{12}(j)z_1z_2+\cdots,\quad j=3,4,5 \tag{3.13}$$

where the ellipsis represents other terms. The derivatives of $z_j$ over $t$ read

$$dz_j/dt\approx 2i\omega B_{11}(j)z_1^2+\cdots,\quad j=3,4,5 \tag{3.14}$$

where we have assumed that $dz_{1,2}/dt\approx\pm i\omega z_{1,2}$.[35] Then, inserting (3.13) and (3.14) into (3.12) and comparing the both sides of the latter for $j=3,4,5$, we have

$$\begin{aligned}
&B_{11}(j)=a_{11}(j)/(-\lambda_j+2i\omega)\ ,\\
&B_{12}(j)=-a_{12}(j)/\lambda_j,\quad j=3,4,5\\
&a_{11}(j)=\beta_{j3}\alpha_{11}\alpha_{51}+\beta_{j4}\alpha_{21}\alpha_{51}-\gamma\beta_{j5}(\alpha_{11}\alpha_{41}+\alpha_{21}\alpha_{51})/2\ ,\\
&a_{12}(j)=\beta_{j3}(\alpha_{12}\alpha_{51}+\alpha_{11}\alpha_{52})+\beta_{j4}(\alpha_{22}\alpha_{51}+\alpha_{21}\alpha_{52})\\
&\qquad-\gamma\beta_{j5}(\alpha_{12}\alpha_{41}+\alpha_{11}\alpha_{42}+\alpha_{22}\alpha_{31}+\alpha_{21}\alpha_{32})/2\ .
\end{aligned}\tag{3.15}$$

Inserting (3.15) into (3.12) for $j=1$ yields the explicit order-parameter equation

$$\begin{aligned}
dz_1/dt=&i\omega z_1+a_{11}(1)z_1^2+a_{12}(1)z_1z_2\\
&+a_{112}(1)z_1^2z_2+\cdots\ ,
\end{aligned}\tag{3.16}$$

where $a_{11}(1)$ and $a_{12}(1)$ are given in (3.15) by taking $j=1$, and the third order coefficient $a_{112}(1)$ can be specified by inserting (3.12) into (3.13) as

$$\begin{aligned}
a_{112}(1)=&\beta_{13}[(\alpha_{11}\alpha_{53}+\alpha_{13}\alpha_{51})B_{12}(3)+(\alpha_{12}\alpha_{53}+\alpha_{13}\alpha_{52})B_{11}(3)+(\alpha_{11}\alpha_{54}+\alpha_{14}\alpha_{51})B_{12}(4)+(\alpha_{12}\alpha_{54}+\alpha_{14}\alpha_{52})B_{11}(4)\\
&\quad+(\alpha_{11}\alpha_{55}+\alpha_{15}\alpha_{51})B_{12}(5)+(\alpha_{12}\alpha_{55}+\alpha_{15}\alpha_{52})B_{11}(5)]\\
&+\beta_{14}[(\alpha_{21}\alpha_{53}+\alpha_{23}\alpha_{51})B_{12}(3)+(\alpha_{22}\alpha_{53}+\alpha_{23}\alpha_{52})B_{11}(3)+(\alpha_{21}\alpha_{54}+\alpha_{24}\alpha_{51})B_{12}(4)+(\alpha_{22}\alpha_{54}+\alpha_{24}\alpha_{52})B_{11}(4)\\
&\quad+(\alpha_{21}\alpha_{55}+\alpha_{25}\alpha_{51})B_{12}(5)+(\alpha_{22}\alpha_{55}+\alpha_{25}\alpha_{52})B_{11}(5)]\\
&-\gamma\beta_{15}\{[(\alpha_{11}\alpha_{43}+\alpha_{13}\alpha_{41})B_{12}(3)+(\alpha_{12}\alpha_{43}+\alpha_{13}\alpha_{42})B_{11}(3)+(\alpha_{11}\alpha_{44}+\alpha_{14}\alpha_{41})B_{12}(4)+(\alpha_{12}\alpha_{44}+\alpha_{14}\alpha_{42})B_{11}(4)\\
&\quad+(\alpha_{11}\alpha_{45}+\alpha_{15}\alpha_{41})B_{12}(5)+(\alpha_{12}\alpha_{45}+\alpha_{15}\alpha_{42})B_{11}(5)]\\
&\quad+[(\alpha_{21}\alpha_{33}+\alpha_{23}\alpha_{31})B_{12}(3)+(\alpha_{22}\alpha_{33}+\alpha_{23}\alpha_{32})B_{11}(3)\\
&\qquad+(\alpha_{21}\alpha_{34}+\alpha_{24}\alpha_{31})B_{12}(4)+(\alpha_{22}\alpha_{34}+\alpha_{24}\alpha_{32})B_{11}(4)+(\alpha_{21}\alpha_{35}+\alpha_{25}\alpha_{31})B_{12}(5)\\
&\qquad+(\alpha_{22}\alpha_{35}+\alpha_{25}\alpha_{32})B_{11}(5)]\}\ .
\end{aligned}\tag{3.17}$$

The calculation is straightforward. By explicitly writing all the terms in $a_{112}(1)$ we want to show that they can, actually, be explicitly given directly in terms of the control parameters. In Eqs. (3.13) and (3.16), the other terms are not explicitly given since they are irrelevant to the discrimination of the nature of bifurcation, which is determined by a quantity $G_3$.[32] (For the mathematical detail we refer readers to Ref. 32 and the references listed there.) $G_3$ for a general system of the form (3.16) is given by[32]

$$G_3=\omega\mathrm{Re}[a_{112}(1)]-\mathrm{Im}[a_{11}(1)a_{12}(1)] \ . \qquad (3.18)$$

So far, the coefficient $G_3$ is given analytically in terms of the control parameters $C$, $k$, $\gamma$, $\theta$, $\Delta$, and $X$ via Eqs. (1.5), (3.6), (3.10), (3.15), and (3.17). The order-parameter equations (2.3) are realized up to the third order.

On the surface $B$, $f=0$, the subset

$$G_3=0$$

is just the codimension-two degenerate Hopf bifurcation set. As $G_3<0$, the surface $B$ indicates supercritical Hopf bifurcation, and then a small-amplitude oscillation can be observed after the stationary solution is destabilized by Hopf bifurcation. In the opposite case $G_3>0$ Hopf bifurcation is subcritical as the surface $B$ is crossed transversally. Thus, the state may, moving far away from the initial steady state, approach other attractors, which may be another branch of the stationary solution, or a new time-dependent solution. In the former case, the state jumps between the two branches of the stationary solution before the turning point is reached; in the latter case, a new attractor of a time-dependent solution coexisting with the stable stationary solution can be predicted. Both discoveries are instructive in the SMOB systems.

In Ref. 12, Erneux and Mandel revealed two kinds of instabilities in SMOB in the limit $C\rightarrow\infty$. They found that for a certain combination of parameters, the stationary solution is replaced by a periodic oscillation when the upper branch is destabilized by Hopf bifurcation. However, the feature of the Hopf bifurcation in the lower branch is rather different from that of the upper one. The system jumps to the upper branch before the turning point is reached whenever Hopf bifurcation takes place. In Ref. 12 this anomalous jumping is specified as a new kind of instability in SMOB. This kind of instability must be a subcritical Hopf instability. When the lower branch is destabilized by an infinitesimal change of the control parameters, the state is repelled far away from the lower branch, and falls into the basin of the attractor of the upper branch. However as we shall show immediately, the attractor eventually reached by the system when subcritical Hopf bifurcation occurs is not necessarily another branch of the stationary solution. It may be some new attractor.

In Fig. 1, at all the points II, type-II bifurcation arises. On the segments $P$ Hopf bifurcation is supercritical, while it is subcritical on $B$.

The most interesting discovery, thanks to the classification of sub- and supercritical bifurcations, can be found in Figs. 3 and 4. In Figs. 3, we consider a parameter combination $C=500$, $k=0.5$, $\gamma=2$, $\theta=-22$, and $\Delta=7.5$ when only a single-valued stationary solution of Eqs. (1.1) exists. By evaluating functions $f$ and $G_3$, it is verified that at $Y_L$ in Fig. 3(a) subcritical bifurcation arises. Hence, it is expected that as $Y<Y_L$, when the unique stationary solution is still stable, there must be a new attractor coexisting with the stable steady solution. The motion on the attractor must be time dependent since no second stable stationary solution exists. In Fig. 3(a), we plot the maximal values of $X$ as a function of the external field. The curve passing $L$ and $U_1$ represents the steady solution which is stable on the solid line while unstable on the dashed one. The two bistability loops are apparent. Between $Y_M$ and $Y_L$ there is a coexistence of a stable stationary solution with an oscillation. Increasing $Y$ from below, the stationary solution loses its stability immediately after $Y_L$ is exceeded. Meanwhile, no characteristic change is observed for the motion on the other attractor at $Y=Y_L$. In Figs. 3(b) and 3(c), we take $Y=516$, which is obviously on the segment $Y_M Y_L$, and plot the evolution of the absolute value of the output as a function of time. In Fig. 3(b), the initial values are given in the vicinity of the steady state; the trajectory approaches the steady state as $t$ increases. On the contrary, in Fig. 3(c) the initial values are given a distance away from the stationary solution; the motion soon turns to be a stable oscillation.

One more remarkable feature arising in Fig. 3(a) is the coexistence of the two time-dependent motions. $Y_{U1}$ is the upper boundary of the Hopf unstable region. At $Y_{U1}$ we have $G_3<0$, then the Hopf bifurcation should be supercritical. Consequently, slightly below $Y_{U1}$ one may expect small-amplitude oscillation. We do find it indeed. Between $Y_{U1}$ and $Y_{U2}$, we again find a coexistence of time-dependent motion and the stable stationary solution. Between $Y_O$ and $Y_{U1}$, the stationary solution is replaced by a small-amplitude oscillation. Hence, a coexistence of two attractors of time-dependent motions is identified. After $Y<Y_O$, the large-amplitude oscillation disappears suddenly. Between $Y_L$ and $Y_O$, there is only a single attractor of periodic motion. In Figs. 3(d) and 3(e), we take $Y=715$. The phase figures are shown in the plane of $\mathrm{Re}(x)$-$\mathrm{Im}(x)$. In Fig. 3(d), the initial state is located in the vicinity of the stationary solution, while in Fig. 3(e) it is far from that. In the former case a small-amplitude periodic trajectory (on the attractor $MU_1$) is identified, while in the latter we find a motion which apparently results from period-doubling bifurcation on the attractor $OU_2$.

In Fig. 4, we take parameter values as $\theta=-18$, $\Delta=6$ with $C$, $k$, and $\gamma$ unchanged from Fig. 3. Then, the stationary solution is triple valued for certain value of $Y$ [see Fig. 4(a)]. The upper (lower) branch is destabilized by super- (sub-) critical Hopf bifurcation at $Y_{U1}$ ($Y_L$) which is shown in Fig. 4(a). Figure 4(a) is similar to Fig. 3(a). Nevertheless, an interesting difference arises after changing the parameters $\theta$ and $\Delta$. Between $Y_{O2}$ and $Y_L$, a coexistence of three attractors, the stable stationary solution, a small-amplitude oscillation, and a large-amplitude oscillation can be observed. Between $Y_{O1}$ and $Y_{U2}$, one again finds a coexistence of three attractors. On the segment $Y_{U1}Y_{U2}$, the coexistence of the stable stationary solution of the upper branch, and two large-amplitude oscillations occurs. On the segment of $Y_{O1}Y_{U1}$, we find a coexistence of three attractors of time-dependent motions. In Figs. 4(b), 4(c), and 4(d), we fix $Y=600$ which is right on $Y_{O1}Y_{U1}$. Starting far away from both the upper and the lower branches initially, we occasionally find Fig. 4(b), which denotes a motion on the attractor $O_2U_3$, or sometimes obtain Fig. 4(c) which is apparently on $O_1U_2$. If the initial state is chosen in the region about the upper branch we grasp a small-amplitude periodic motion which results from the destabilization of the upper branch via the supercritical Hopf bifurcation (on $MU_1$).

It is noticed that in Figs. 3(a) and 4(a), the curves look

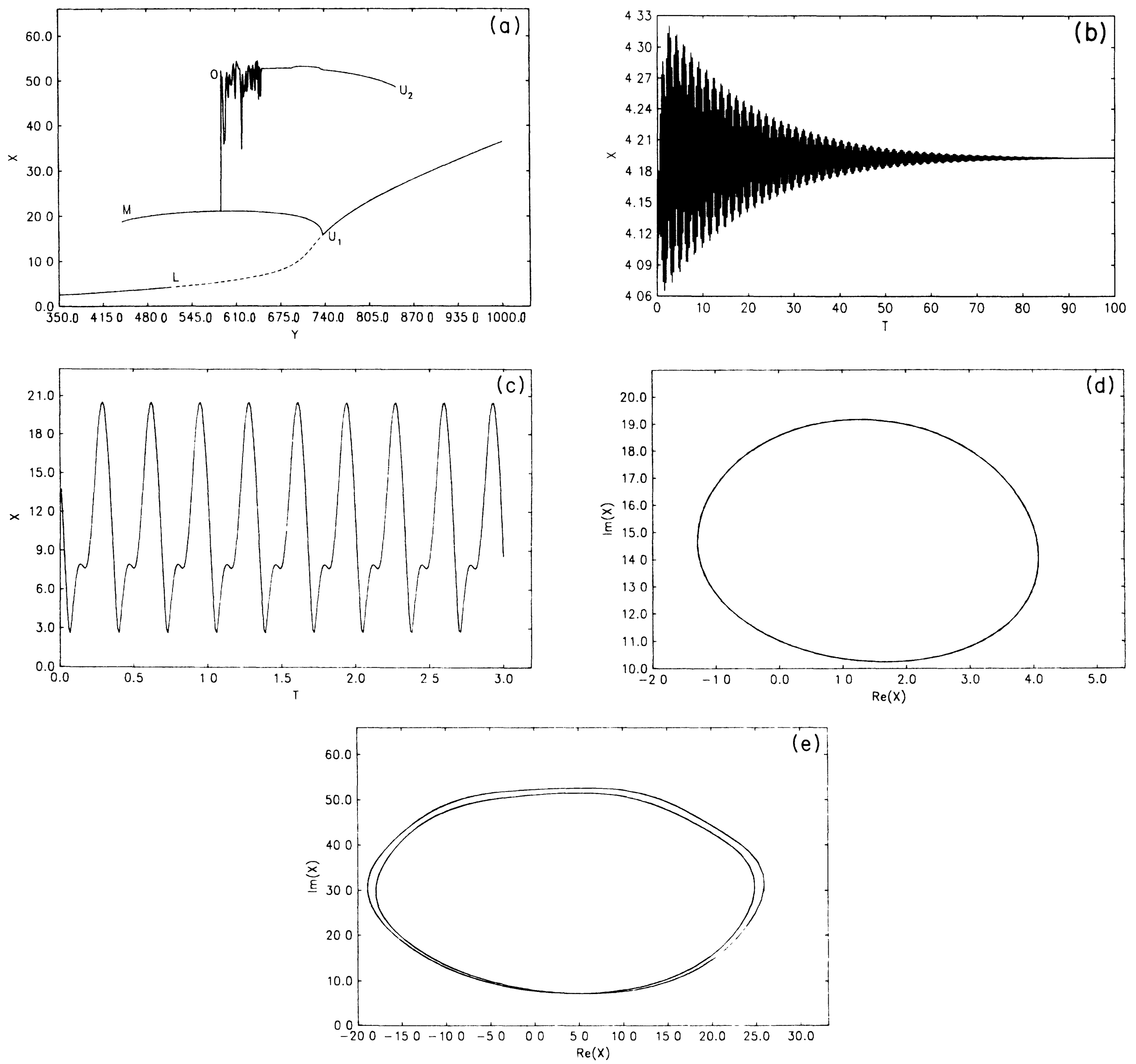


FIG. 3. (a) $C=500$, $\theta=-22$, $\Delta=7.5$, $k=0.5$, and $\gamma=2$. The stationary solution is single valued. The $x$ coordinate represents the maximal value of $X$ (the transcient process has been excluded). A new attractor on which a large amplitude oscillation occurs is observed. Two bistability loops are apparent. (b) $Y=516$. The other parameters are the same as in (a). The initial state is near the steady state. The system quickly relaxes to the steady state. (c) The parameters chosen are the same as in (b). The initial state is far from the stationary solution. The system finally approaches a periodic motion. (d) The parameters are given in (a) with $Y=715$. The initial values are provided in the vicinity of the steady state. The system ends up with a small-amplitude oscillation. (e) All parameters are of the same values as in (d). The initial state is far away from the steady state. The system is finally attracted by a double-periodic oscillation.

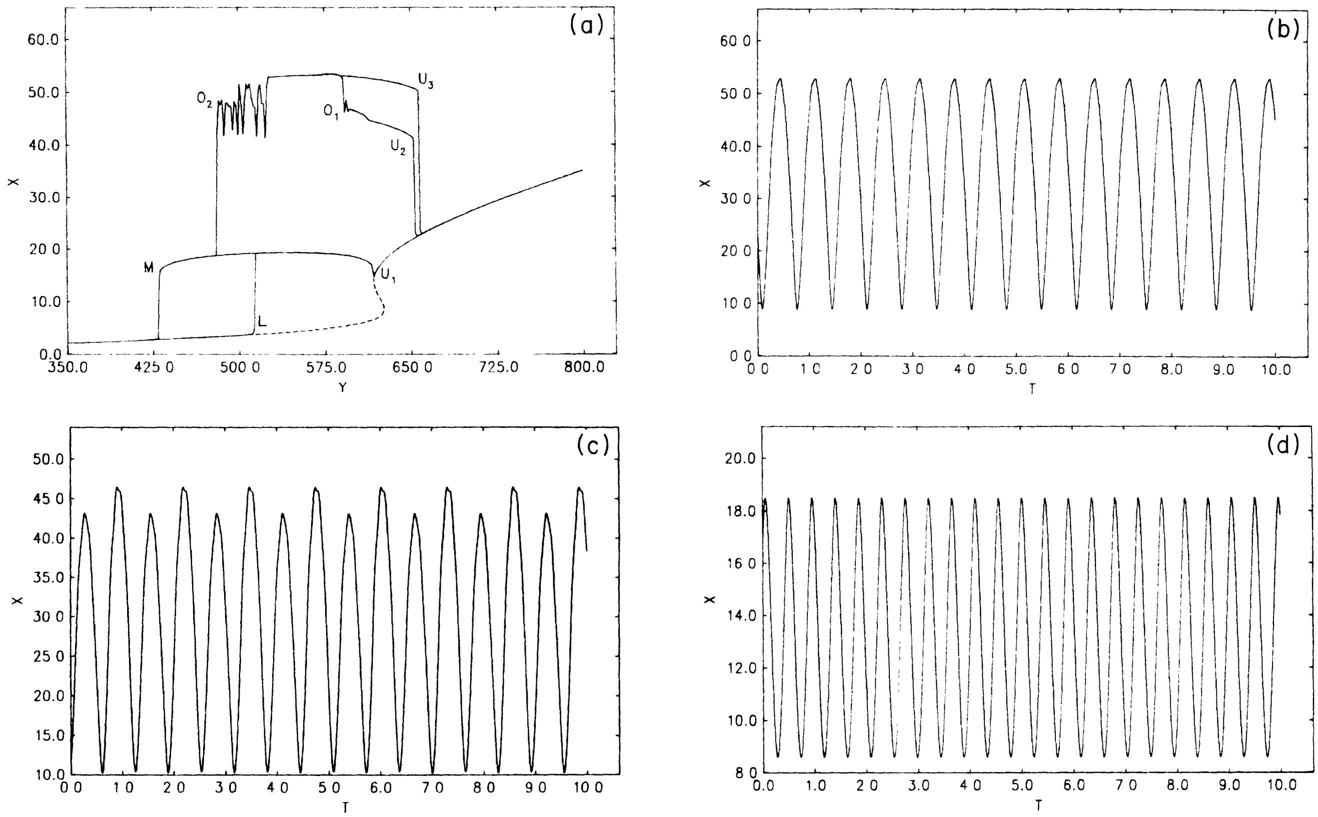


FIG. 4. (a) The parameters and the meanings of the curves are the same as in Fig. 3(a) with $\theta$ and $\Delta$ replaced by $-18$ and 6, respectively. Tristability can be found in the regions $Y_{O2}Y_L$ and $Y_{O1}Y_{U2}$. (b) The parameters are the same as in (a) with $Y=600$ where tristability of oscillation occurs. For certain initial conditions the system approaches this large-amplitude oscillation which is on $O_2U_3$ in (a). (c) When the initial condition is changed from those of (b) the system may occasionally end up with a double-period oscillation which is on the attractor $O_1U_2$ in (a). (d) When the initial condition is chosen very close to the steady state, the system finally reaches a small-amplitude oscillation on the attractor $MU_1$.

irregular after $Y_O$ [Fig. 3(a)] or $Y_{O2}$ [Fig. 4(a)]. The motion on those parameter regions may be expected to be complicated. In fact, we have indeed found aperiodic motion in these regions. However, we do not intend to go further into this matter in the present paper.

We would like to emphasize that apart from what we have shown in Figs. 3 and 4, there is still a variety of behaviors of the motion after the stationary state is destabilized by Hopf bifurcation. In Fig. 1, for instance, if we fix $\Delta=6.19$, the entire Hopf unstable region falls into the lower branch of the stationary solution. (This phenomenon is seldom observed. There exists an island of the Hopf unstable region while the segment of the lower branch near the turning point remains stable. Even in Fig. 1 this phenomenon can be found only for a very small interval of $\Delta$.) For the given parameters, both Hopf bifurcations on the lower branch are supercritical. After the stationary solution is destabilized by Hopf bifurcation, no jump to the upper branch occurs. Instead, the stationary solution is replaced by a small-amplitude periodic motion which can be seen in Fig. 5. [In Fig. 5, the meaning of the curves is the same as in Figs. 3(a) and 4(a).] If we fix $\Delta=3.03$, the bifurcation figure is completely different. Then, on both the upper and lower branches the Hopf bifurcations are subcritical. A jump to the upper stable stationary solution does happen as the lower branch is destabilized by the Hopf bifurcation before reaching the turning point; it is just the kind of bifurcation explored in Ref. 12. Meanwhile, as the upper branch is destabilized, a large-amplitude oscillation bursts, replacing the unstable stationary solution of the upper branch.

## IV. CONCLUDING REMARKS

Let us end our presentation by offering the following remarks.

(i) For the first time, we have detailed the conditions of codimension-two bifurcations of SMOB modeled by Eqs. (1.1). We believe that codimension-two bifurcations are the most important multicodimension bifurcations in SMOB which really give physical effects. Based on the understanding of type-III B bifurcation, one may expect to analytically predict the onset of chaos, and on that of type-II bifurcation, new attractors may be explored in a systematic way.

(ii) In Sec. III, we have indeed found several kinds of new attractors which have never been reported for SMOB. A time-dependent solution may be found in the

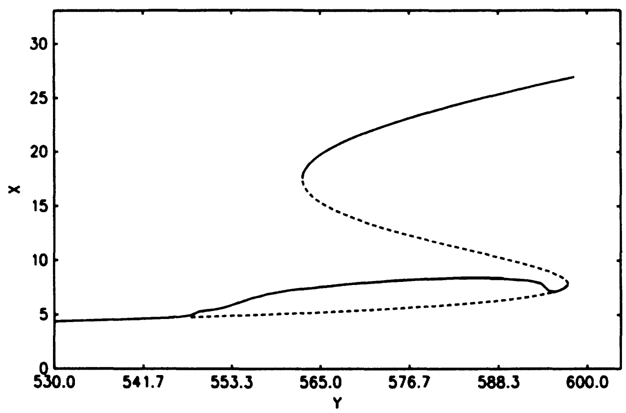


FIG. 5. The maximal values of $X$ are plotted against $Y$ after the system eventually reaches its asymptotic state. $\Delta=6.19$. All the other parameters are given in Fig. 1. Both bifurcations at the two boundaries of the Hopf unstable region on the lower branch are supercritical. A small-amplitude oscillation arises immediately after the stationary solution is destabilized by Hopf bifurcation.

parameter region where the stationary solution keeps its stability. Moreover, the coexistence of three attractors is a rather interesting discovery. In Figs. 3(a) and 4(a), we demonstrate the existence of an attractor of large-amplitude oscillation. This new attractor can be observed in a wide parameter region. It seems to us that the complicated motion revealed for the SMOB system may be related to the motion on this attractor.

(iii) The approach used in the present work can be directly extended to laser systems with an active medium by taking $\sigma=-1$ instead of $\sigma=1$. In the case of $\sigma=-1$, $Y=0$, and $\theta=\Delta=0$, we go back to the FRL system, or equivalently, the standard Lorenz equations.

(iv) In Ref. 12 it was found that the Hopf bifurcation instability in the lower branch will lead to the earlier switching to the upper state. As these authors remark their analysis cannot answer the question whether the bifurcation can lead to stable oscillation or not. Our analysis, together with those in Refs. 17, 12, and 37, shows that four outcomes of the low-branch instability exist. Apart from the anomalous switching as studied in Refs. 17 and 37, which is essentially a kind of global instability and does not require the local instability, the instability can also lead to a small-amplitude oscillation (supercritical case) as shown in Fig. 5, to a finite-amplitude oscillation (in some cases of subcriticality), as shown in Figs. 3(a) and 4(a), or to an earlier switching due to a Hopf bifurcation instability (in other cases of subcriticality). Therefore a complete understanding of the low-branch instability is reached.

*Permanent address: Department of Physics, Beijing Normal University, Beijing, China.

[1]H. Haken, Phys. Lett. **53A**, 77 (1975).
[2]R. Graham and H. Haken, Z. Phys. **312**, 420 (1968).
[3]H. Risken and K. Nummedal, Phys. Lett. **26A**, 275 (1968).
[4]M. Mayr, H. Risken, and D. Vollmer, Opt. Commun. **36**, 480 (1981).
[5]L. A. Lugiato, Nuovo Cimento Lett. **33**, 609 (1978).
[6]L. A. Lugiato, L. M. Narducci, D. K. Bandy, and C. A. Pennise, Opt. Commun. **46**, 64 (1983).
[7]K. Ikeda, H. Daido, and O. Akomoto, Phys. Rev. Lett. **45**, 709 (1980).
[8]K. Ikeda and O. Akomoto, Phys. Rev. Lett. **48**, 617 (1982).
[9]L. A. Lugiato, R. J. Horowicz, and G. Strini, Phys. Rev. A **30**, 1366 (1984).
[10]L. A. Lugiato and L. M. Narducci, Phys. Rev. A **32**, 1576 (1985).
[11]L. M. Narducci, J. R. Tredicce, L. A. Lugiato, N. B. Abraham, and D. K. Bandy, Phys. Rev. A **32**, 1588 (1985).
[12]T. Erneux and P. Mandel, Phys. Rev. A **33**, 1777 (1986).
[13]L. A. Lugiato, in *Progress in Optics,* edited by E. Wolf (North-Holland, Amsterdam, 1984), Vol. XXI.
[14]R. Bonifacio and P. Meystre, Opt. Commun. **29**, 131 (1979).
[15]V. Benza and L. A. Lugiato, Nuovo Cimento Lett. **26**, 405 (1979).
[16]P. D. Drummond, Opt. Commun. **40**, 224 (1982).
[17]F. A. Hopf, P. Meystre, P. D. Drummond, and D. F. Walls, Opt. Commun. **31**, 245 (1979).
[18]L. A. Lugiato and R. Lefever, Phys. Rev. Lett. **58**, 2209 (1987).
[19]J. Y. Zhang, H. Haken, and H. Ohno, J. Opt. Soc. Am. B **2**, 141 (1985).
[20]G. Hu and G. J. Yang, Phys. Rev. A **38**, 1979 (1988).
[21]G. J. Yang and G. Hu, Phys. Rev. A **39**, 2514 (1989).
[22]J. E. Marsden and M. McCracken, *The Hopf Bifurcation and its Application,* Vol. 19 of *Applied Mathematical Sciences,* edited by F. John, L. Sirovich, and J. P. LaSalle (Springer, Berlin, 1976).
[23]G. Tsarouhas and J. Pade, Physica **138A**, 507 (1986).
[24]C. Z. Ning and H. Haken, Z. Phys. B **77**, 163 (1989).
[25]G. Dangelmayr, M. Neveling, and D. Armbruster, Z. Phys. B **64**, 491 (1986); **59**, 365 (1985).
[26]H. Haken and H. Ohno, Opt. Commun. **16**, 205 (1976); **26**, 117 (1978).
[27]F. Takens, Publ. Inst. Hautes Études Sci. Paris **43**, 47 (1974).
[28]V. I. Arnold, Russ. Math. Surv. **27**, 54 (1972).
[29]J. Guckenheimer and P. Holmes, *Nonlinear Oscillations, Dynamical Systems, and Bifurcations of Vector Fields* (Springer-Verlag, New York, 1983), pp. 352–412.
[30]H. Haken, *Synergetics, an Introduction,* 3rd ed. (Springer, New York, 1983).
[31]H. Haken, *Advanced Synergetics* (Springer, New York, 1987).
[32]C. Z. Ning, J. Phys. A: Math. Gen. **21**, L491 (1988).
[33]C. Z. Ning and H. Haken, Phys. Rev. A (to be published).
[34]G. Hu and H. Haken, Phys. Rev. A **40**, 1899 (1989).
[35]H. Haken, *Light, Vol. 2—Laser Light Dynamics* (North-Holland, Amsterdam, 1985); H. Haken and H. Ohno, Opt. Commun. **16**, 205 (1976).
[36]G. Hu and G. J. Yang, Phys. Rev. A **40**, 834 (1989).
[37]L. A. Lugiato, M. Milani, and P. Meystre, Opt. Commun. **40**, 307 (1982); T. Erneux and P. Mandel, in *Optical Bistability III,* edited by H. M. Gibbs *et al.* (Springer, Berlin, 1986).